

Observation of Weak Impact of a Stochastic Magnetic Field on Fast-Ion Confinement

G. Fiksel, B. Hudson, D. J. Den Hartog, R. M. Magee, R. O'Connell, and S. C. Prager

Department of Physics, University of Wisconsin—Madison and Center for Magnetic Self Organization in Laboratory and Astrophysical Plasmas, Madison, Wisconsin 53706, USA

A. D. Beklemishev, V. I. Davydenko, A. A. Ivanov, and Yu. A. Tsidulko

Budker Institute of Nuclear Physics, Novosibirsk, Russia

(Received 17 May 2005; published 14 September 2005)

Fast ions are observed to be very well confined in the Madison Symmetric Torus reversed field pinch despite the presence of stochastic magnetic field. The fast-ion energy loss is consistent with the classical slowing down rate, and their confinement time is longer than expected by stochastic estimates. Fast-ion confinement is measured from the decay of d - d neutrons following a short pulse of a 20 keV atomic deuterium beam. Ion confinement agrees with computation of particle trajectories in the stochastic magnetic field, and is understood through consideration of ion guiding center islands.

DOI: [10.1103/PhysRevLett.95.125001](https://doi.org/10.1103/PhysRevLett.95.125001)

PACS numbers: 52.50.Gj, 52.20.Dq, 52.25.Xz

Magnetic fields can be stochastic in numerous laboratory and astrophysical plasmas. The trajectories of charged particles can then also be stochastic, with a large effect on particle transport. The diffusion of the magnetic field in space can be characterized by a diffusion coefficient, D_m . For particles that are closely tied to field lines, a simple estimate for particle diffusion in a stochastic field is [1] $D \sim \nu D_m$, where ν is the particle velocity along the field. However, for energetic (fast) particles, guiding center drifts can cause the particle path to differ significantly from the field line path, and the influence of field stochasticity on transport becomes less clear. Energetic particle transport in a stochastic magnetic field is influential for laboratory plasmas studied for fusion energy; for example, it will affect the feasibility of neutral beam injection as a means to heat the plasma and will determine the confinement of fusion produced alpha particles during magnetic reconnection. For astrophysical plasmas, energetic particle transport in stochastic fields can be important in thermal conduction in galaxy-cluster plasmas and cosmic ray propagation.

In this Letter, the reversed field pinch (RFP) laboratory plasma is employed to measure transport of fast particles in a stochastic magnetic field of a standard RFP plasma. We measure the confinement of fast ions generated by injection of energetic neutral atoms. The confinement is determined through detection of neutrons from the fusion reaction between the fast ions and the background deuterium plasma.

Electrons, which are closely tied to field lines, have been shown previously [2–6] to obey the above estimate for confinement. We show here that the transport of energetic ions is far below that estimate: the ion orbits are well ordered, despite the stochasticity of the underlying magnetic field. However, if the stochasticity becomes sufficiently large—as occurs during a reconnection event—the ion confinement is degraded. These results are understood theoretically by applying ideas commonly employed

for magnetic fields to the ion guiding center trajectories. The helical trajectories of the ion guiding center in the equilibrium magnetic field can be described by a rotational transform. When perturbed, the ion trajectories can develop islands, which can overlap and lead to stochasticity and transport [7]. These ideas have been confirmed through numerical simulation of ion trajectories. The condition for island overlap for ion guiding centers differs from that for magnetic field lines. Hence, we observe that fast-ion confinement far exceeds that expected for low energy ions, a favorable result for the application of neutral beam injection for the RFP. However, during a reconnection event, the magnetic stochasticity becomes sufficiently large that the ion transport increases dramatically.

In the Madison Symmetric Torus (MST) RFP [8] (with minor radius $a = 0.51$ m, major radius $R = 1.5$ m) fast-ion confinement is measured via decay of d - d fusion 2.5 MeV neutrons following a short pulse of an atomic deuterium beam injected into the deuterium plasma. This technique was successfully applied for fast-ion confinement studies in tokamaks [9,10], spherical tori [11], helical systems [12], and mirror machines [13]. The RFP introduces the new element of magnetic stochasticity.

A short pulse (1.3 ms) of deuterium atoms at an energy of 20 keV (0.5 MW) was injected approximately at the equatorial plane, tangential to the magnetic axis, and parallel to the toroidal plasma current. The beam content of particles with the full energy is greater than 90%. The neutron flux was measured with a plastic scintillator (Bicron BC-408), 127 mm (5 in.) in diameter and 127 mm (5 in.) in length, coupled with a 130 mm diameter photomultiplier tube, both shielded from hard x rays by 5 cm thick lead, and placed near the MST vacuum vessel.

The measurements were performed in “standard” RFP plasmas, which are inhabited by multiple modes of internally resonant tearing magnetic fluctuations, magnetic field stochasticity, and a particle confinement time about

1 ms [4,14]. For these experiments, the plasma current $I_p = 400$ kA, central plasma density $n_0 \approx 1.2 \times 10^{13}$ cm $^{-3}$, and the central electron temperature $T_{e0} = 400$ eV. The electron density profile was measured with an 11-chord far infrared interferometer [15] and the electron temperature profile with a multipoint Thomson scattering system.

The flux of neutrons (Fig. 1) increases during beam injection, from the buildup of the fast ions. Thereafter it slowly decays in several milliseconds. If we assume a slowing down of ions by classical Coulomb collisions, then from the data of Fig. 1 we can determine the fast-ion confinement time.

The total neutron flux is calculated from

$$\Gamma_n(t) = \int_V n_i(\mathbf{r}) n_{fi}(\mathbf{r}, t) \sigma_T(E_{fi}(t)) v_{fi}(t) dV, \quad (1)$$

where $\sigma_T(E_{fi})$ is the d - d fusion cross section [16] and n_{fi} is the fast-ion density. We model the fast-ion energy losses by the classical collisional rate [17]:

$$\frac{1}{E_{fi}} \frac{dE_{fi}}{dt} = - \frac{Z_{fi}^2 e^4 n_e m_{fi}^{1/2} \ln \Lambda}{4\sqrt{2}\pi \epsilon_0^2 m_e E_{fi}^{3/2}} \times \left[\frac{4}{3\pi^{1/2}} \left(\frac{m_e}{m_{fi}} \frac{E_{fi}}{T_e} \right)^{3/2} + \sum_i \frac{m_e}{m_i} \frac{n_i Z_i^2}{n_e} \right], \quad (2)$$

where E_{fi} and m_{fi} are the fast-ion energy and mass, and the remaining notation is standard. The right-hand side includes slowing from electrons and ions. The plasma mean ion charge was assumed $Z_{eff} = 2$ with C^{6+} being the main impurity. The uncertainty in Z_{eff} does not affect our conclusions.

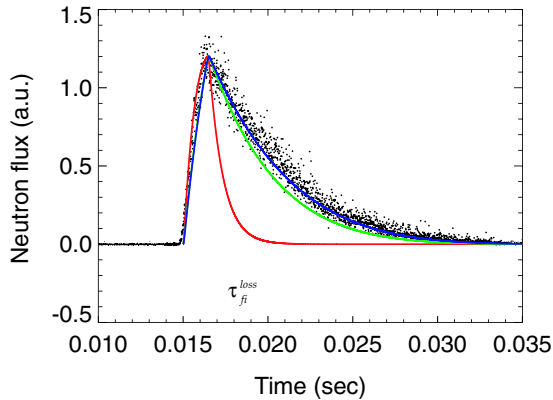


FIG. 1 (color online). Comparison of measured neutron signal (dots) and modeling (solid lines). The shaded area represents the NBI duration. The solid $\tau_{fi}^{loss} = \infty$ line is a result of modeling with classical fast-ion slowing down and perfect ion confinement. The vertical error bars represent the spread due to statistical uncertainty in T_e measurements. The solid $\tau_{fi}^{loss} = 20$ ms and $\tau_{fi}^{loss} = 1$ ms lines show the fits for the corresponding fast-ion confinement times.

The fast-ion density profile at birth is calculated numerically by tracking the fast ions and computing the time spent at each point. The ion orbits were calculated using full orbit equations with equilibrium magnetic field profiles obtained using an equilibrium reconstruction code [18]. The contributions from the ions born at different points along the primary beam were weighted according to the beam attenuation. The resulting density profile is peaked at the plasma center with about 70% of the fast particles contained inside $r/a = 0.3$.

We assume that the fast-ion profile does not change in time during the neutron decay. This assumption is justified *a posteriori* by the large fast-ion confinement time. Furthermore, we confirmed that *ad hoc* changes in the fast-ion profile do not change significantly the neutron yield because of the relative flatness of n_e and T_e profiles. We assume that the fast-ion losses can be described by a single time constant τ_{fi}^{loss} according to

$$\frac{dn_{fi}}{dt} = S_{fi} - \frac{n_{fi}}{\tau_{fi}^{loss}}, \quad (3)$$

where S_{fi} is the known fast-ion source. Equations (1)–(3) are solved simultaneously to infer τ_{fi}^{loss} .

The calculated neutron flux time history for different values of τ_{fi}^{loss} is shown in Fig. 1 (solid lines). The calculated neutron flux is normalized to the experimental value at the end of injection. The curve with the fast-ion confinement time $\tau_{fi}^{loss} = 20$ ms lies below the experimental points, and the curve corresponding to the stochastic confinement time $\tau_{fi}^{loss} = 1$ ms decays much faster than the experimental data. Therefore, confinement is much longer than predicted by the simple stochastic estimate and is bounded from below by 20 ms.

To compare with experiment we compute ion trajectories in the magnetic field using the code RIO which resolves full ion orbits in a magnetic field. Helical magnetic perturbations with poloidal mode numbers $m = 0, 1$ and toroidal mode numbers from $n = 1$ –32 that are dominant in MST are included. The radial profiles of each tearing mode Fourier harmonic fluctuation were computed by a non-linear resistive MHD code DEBS [19], and the amplitudes were normalized to the corresponding values measured at the MST wall. The energy losses in the background plasma are represented by the friction force $(\nu_s^e + \nu_s^i) \mathbf{v}_{fi}$, which includes the fast-ion slowing down on plasma electrons and ions. The velocity pitch angle scattering and diffusion are small relative to slowing down and were neglected.

Figure 2(a) illustrates the difference between the ion guiding center orbits and the field lines, which are shown for the same starting point, $r/a = 0.15$. Energy losses were neglected for clarity. Ion orbits stay attached to the starting flux surface, but the field lines quickly diffuse in the radial direction and exhibit stochastic behavior. The difference arises since orbit drifts modify the resonance coupling to

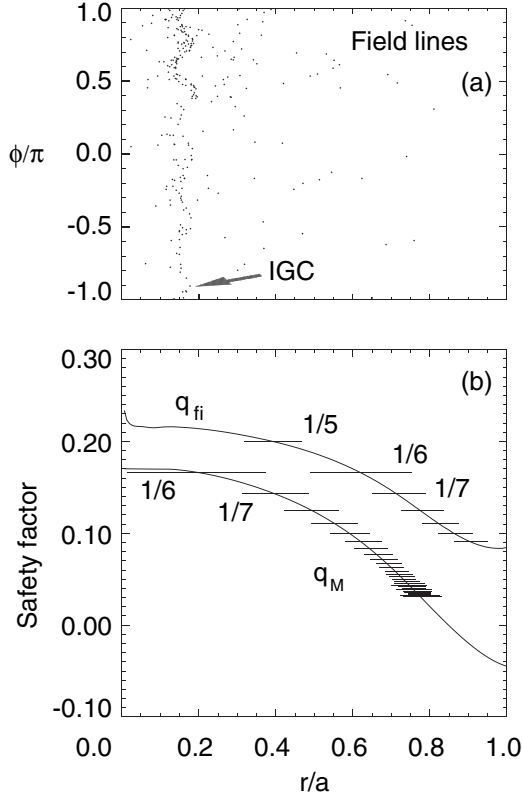


FIG. 2. (a) Puncture plots, in the radius-toroidal angle (r - ϕ) plane, of magnetic field line and ion guiding center (IGC) with the same starting point $r/a = 0.15$. The field line randomly wanders through the plasma volume while the fast ion stays attached to a flux surface. (b) Safety factor profile for magnetic lines (q_M) and for fast ions guiding center (q_{fi}). The horizontal lines depict the positions of resonant surfaces $q = m/n$ and the widths of the corresponding magnetic islands.

the magnetic field perturbations in the way illustrated in Fig. 2(b).

Figure 2(b) depicts the profile of the magnetic field safety factor $q_M = rB_\phi/RB_\theta$ and the position of tearing resonances $q_M(r) = m/n$. The $m = 1$ magnetic island widths for the dominant modes, calculated as $w_M = 4\sqrt{\frac{\tilde{v}_{rn}}{B_\theta} \frac{r}{nq_M}}$ [20], are indicated by straight lines. The innermost island corresponds to the $n = 6$ mode resonant at $q_M = 1/6$. The $n = 5$ mode is not resonant since $q_M < 1/5$. The observed overlapping of the magnetic islands is the cause for magnetic field stochasticity.

The ion orbits have a rotational transform different from that of the field lines, which changes the resonant interaction with the magnetic fluctuations. In analogy to the magnetic field safety factor we can define, in the drift approximation, the “ion guiding center (IGC) safety factor” as $q_{fi} = rv_\phi/Rv_\theta$, where v_ϕ and v_θ are toroidal and poloidal guiding center velocities. They are not equal, $q_{fi} \neq q_M$, because $v_\phi/v_\theta \neq B_\phi/B_\theta$ due to the ion orbit drift. The IGC safety factor profile is shown in Fig. 2(b) for

a D^+ ion with an energy 20 keV and a starting point $r/a = 0.15$. Following the magnetic field analogy one can calculate the “IGC island width”: $w_{fi} = 4\sqrt{\frac{\tilde{v}_{rn}}{v_\theta} \frac{r}{nq_{fi}}}$, where \tilde{v}_{rn} is the radial component velocity resonant with q_{fi} and the resulting IGC islands are depicted in Fig. 2(b). Since the q_{fi} profile is shifted upward relative to the q_M profile, the $q_{fi} = 1/6$ resonance is displaced to $r/a = 0.6$, and a new resonance $q_{fi} = 1/5$ appears at $r/a = 0.4$. The innermost IGC islands do not overlap and the central region is resonance-free, which explains the good ion confinement.

The dynamical evolution as the fast ions slow down is shown in Fig. 3. The ion energy decays according to the collisional slowing down rate [Fig. 3(a)] while the position of the ion guiding center [Fig. 3(b)] remains attached to a flux surface, until the energy reaches a threshold value (≈ 7 keV for a D ion) at $t = 0.016$ s at which point the ion trajectory becomes stochastic. This agrees with an expectation that at sufficiently low energy the ion trajectory approaches the field line and replicates its stochastic properties. Indeed, calculations show that as the fast-ion energy decreases so does the gap between the fast-ion q_{fi} and the magnetic q_M profiles; at the threshold energy the IGC islands overlap, triggering stochasticization of the ion orbits. The threshold energy corresponds to a relative value of the ion Larmor radius $\rho_L/a \approx 0.05$. The jump in the ion guiding center position at $t = 0.007$ s in Fig. 3(b) corresponds to the trapping of the ion in the $q_{fi} = 1/5$ island as the ion slows.

If the magnetic stochasticity becomes sufficiently large, then even particles with large guiding center drifts can develop stochastic trajectories and large transport. During a reconnection event in MST, the magnetic fluctuation

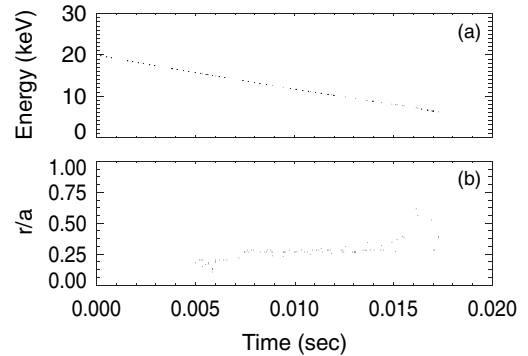


FIG. 3. (a) Time dependence of ion energy and (b) the position of the ion guiding center obtained with the code RIO. The ion remains attached to a flux surface until the energy reaches a threshold value (≈ 7 keV for a D ion) at $t = 0.016$ s at which point the ion trajectory becomes stochastic. A characteristic jump in the ion guiding center position at $t = 0.007$ s corresponds to trapping of the ion into the $q_{fi} = 1/5$ island as the island moves towards the plasma center during the slowing down. The threshold energy corresponds to the Larmor radius $\rho_L/a \approx 0.05$.

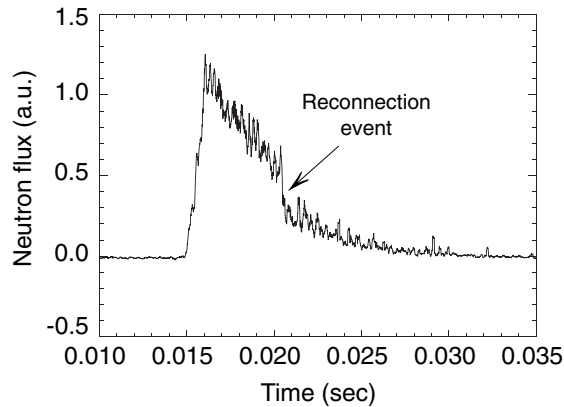


FIG. 4. Waveform of neutron flux with a reconnection event at $t = 0.02$ s. During the $\sim 200 \mu\text{s}$ duration of the event, the neutron flux drops by a factor of 2. After the event the slow decay is resumed.

amplitudes triple, and we calculate that the ion guiding centers should overlap, leading to stochasticity. We observe that the neutron flux halves during the $200 \mu\text{s}$ reconnection event (corresponding to the crash phase of a sawtooth oscillation), as shown in Fig. 4. This indicates that the fast-ion confinement decreases from more than 20 ms to of the order of $200 \mu\text{s}$ during the reconnection event.

In summary, confinement of fast ions in the stochastic magnetic field of the RFP was studied by measuring the decay of the fusion $d-d$ neutron flux following impulsive injection of deuterium neutrals. The fast-ion confinement time (>20 ms) is much longer than the estimate for lower energy particles that closely follow field lines (~ 1 ms), and also longer than the bulk plasma confinement time (~ 1 ms). This relative immunity of fast ions to field stochasticity agrees with the computation of particle orbits in the RFP stochastic field, and is understood from inspection of ion guiding center islands, which can differ significantly from magnetic islands. However, during a reconnection event, stochasticity is sufficiently large that fast-ion trajectories become stochastic and the confinement time decreases (to $\sim 200 \mu\text{s}$). These results illustrate the limits of the simple transport estimates that assume that particles follow field lines. They also show that fast ions are well confined in the RFP, a favorable result for the use of neutral beam injection as a control tool, and for confinement of fusion-generation alpha particles. For the latter, the observed threshold transition to poor confinement at low energy can possibly be exploited as a means for “ash” removal.

The work was supported by the U.S. Department of Energy. The authors are thankful to V. Ya. Savkin and A. V. Sorokin for help with the neutral beam injector and

to J. Sarff, D. Craig, and B. Chapman for stimulating discussions and suggestions. One of the authors (G.F.) acknowledges very useful discussions with W. W. Heidbrink.

-
- [1] A. B. Rechester and M. N. Rosenbluth, *Phys. Rev. Lett.* **40**, 38 (1978).
 - [2] G. Fiksel, S. C. Prager, W. Shen, and M. Stoneking, *Phys. Rev. Lett.* **72**, 1028 (1994).
 - [3] G. Serriani, A. Murari, G. Fiksel, V. Antoni, M. Bagatin, D. Desideri, E. Martines, and L. Tramontin, *Plasma Phys. Controlled Fusion* **43**, 919 (2001).
 - [4] T. M. Biewer, C. B. Forest, J. K. Anderson, G. Fiksel, B. Hudson, S. C. Prager, J. S. Sarff, and J. C. Wright, *Phys. Rev. Lett.* **91**, 045004 (2003).
 - [5] M. R. Stoneking, S. A. Hokin, S. C. Prager, G. Fiksel, H. Ji, and D. J. Den Hartog, *Phys. Rev. Lett.* **73**, 549 (1994).
 - [6] R. O’Connell, D. J. Den Hartog, C. B. Forest, J. K. Andersen, T. M. Biewer, B. E. Chapman, D. Craig, G. Fiksel, S. C. Prager, J. S. Sarff, S. D. Terry, and R. W. Harvey, *Phys. Rev. Lett.* **91**, 045002 (2003).
 - [7] S. V. Putvinskii, in *Review of Plasma Physics*, edited by B. B. Kadomtsev (Consultants Bureau, New York, London, 1993), Vol. 18.
 - [8] R. N. Dexter, D. W. Kerst, T. W. Lovell, S. C. Prager, and J. C. Sprott, *Fusion Technol.* **19**, 131 (1991).
 - [9] W. W. Heidbrink and G. J. Sadler, *Nucl. Fusion* **34**, 535 (1994).
 - [10] K. Tobita, K. Tani, T. Nishitani, K. Nagashima, and Y. Kusama, *Nucl. Fusion* **34**, 1097 (1994).
 - [11] W. W. Heidbrink, M. Miah, D. Darrow, B. LeBlanc, S. S. Medley, A. L. Roquemore, and F. E. Cecil, *Nucl. Fusion* **43**, 883 (2003).
 - [12] M. Isobe, M. Sasao, M. Osakabe, M. Fujita, S. Okamura, R. Kumazawa, and T. Minami, *Rev. Sci. Instrum.* **68**, 532 (1997).
 - [13] V. V. Maximov, A. V. Anikeev, P. A. Bagryansky, A. A. Ivanov, A. A. Lizunov, S. V. Murakhtin, K. Noack, and V. V. Prikhodko, *Nucl. Fusion* **44**, 542 (2004).
 - [14] B. E. Chapman, A. F. Almagri, J. K. Anderson, and T. M. Biewer, *Phys. Plasmas* **9**, 2061 (2002).
 - [15] D. L. Brower, W. X. Ding, S. D. Terry, J. K. Anderson, T. M. Biewer, B. E. Chapman, D. Craig, C. B. Forest, S. C. Prager, and J. S. Sarff, *Rev. Sci. Instrum.* **74**, 1534 (2003).
 - [16] H.-S. Bosch and G. M. Hale, *Nucl. Fusion* **32**, 611 (1992).
 - [17] K. Miyamoto, *Plasma Physics for Nuclear Fusion* (MIT Press, Cambridge, MA, 1989).
 - [18] J. K. Andersen, C. B. Forest, T. M. Biewer, J. S. Sarff, and J. C. Wright, *Nucl. Fusion* **44**, 162 (2004).
 - [19] D. D. Schnack, D. C. Barnes, Z. Mikic, D. S. Harned, and E. J. Caramana, *J. Comput. Phys.* **70**, 330 (1987).
 - [20] A. J. Lichtenberg and M. A. Lieberman, *Regular and Stochastic Motion* (Springer-Verlag, New York, 1983).